MATERIALS PHYSICS AND MECHANICS RESEACH ARTICLE

Submitted: August 8, 2023 Revised: September 11, 2023 Accepted: December 6, 2023

Impact of non-local, two temperature and impedance parameters on propagation of waves in generalized thermoelastic medium under modified Green-Lindsay model

S. Kaushal [1✉], **R. Kumar** [2], **I. Bala** [1], **G. Sharma** [1,3]

[1] Lovely Professional University, Phagwara, India

[2] Kurukshetra University, Haryana, India

[3] Doaba College, Jalandhar, India

✉ sachin_kuk@yahoo.co.in

ABSTRACT

This study is primarily focused on the behavior of propagation of waves through a homogeneous and isotropic thermoelastic half-space using the modified Green-Lindsay theory of thermoelasticity, along with the effects of non-local and two temperature (TT) parameters. A new set of governing equations is formulated and solved using the reflection technique after reducing the equations to two dimensions and a dimensionless form. The impact of different parameters namely non-local parameter, TT parameter, and impedance parameters along with different theories of thermoelasticity are shown graphically on amplitude ratios obtained from reflected waves i.e., longitudinal wave (LD-wave), thermal wave (T-wave), and transverse wave (SV-wave). The modified Green-Lindsay theory is widely used in fields such as heat transfer, and geophysics with potential practical applications in areas such as earthquake engineering and materials engineering. The study also includes the deduction of particular cases based on the obtained results.

KEYWORDS

modified Green-Lindsay theory • non-local • two temperature • impedance parameters

Citation: Kaushal S, Kumar R, Bala I, Sharma G. Impact of non-local, two temperature and impedance parameters on propagation of waves in generalized thermoelastic medium under modified Green-Lindsay model. *Materials Physics and Mechanics*. 2024;52(1): 1–17.

http://dx.doi.org/10.18149/MPM.5212024_1

Introduction

The mathematical framework known as the two temperature (TT) theory of thermoelasticity describes how materials respond to thermal loads and is an extension of the classical theory of elasticity. This theory finds use in several engineering disciplines that depend on the system's performance under thermal loads. For instance, in the semiconductor industry, the two temperature theory can be used to model electronic device behavior at elevated temperatures. Many authors have discussed different types of problems in the context of theory of thermoelasticity notable of them are [1–5].

Youssef [6] proposed a novel model of generalized thermoelasticity by incorporating two distinct temperatures, namely thermodynamic temperature and conductive temperature. Later on, [7–10] explored different types of problems in the context of TT theory of elasticity. Lofty et al. [11] established a memory-depended derivative (MDD) during the excitation processes by pulsed laser for a time-dependent material under the magneto thermoelasticity with TT. Al-Lehaibi [12] discussed the

Publisher: Peter the Great St. Petersburg Polytechnic University

variational principle theorem without energy dissipation for an isotropic and homogeneous material in the context of the TT theory of thermoelasticity.

Green and Lindsay's (G-L) theory assumes linear behavior of the material, meaning that the response is assumed to be proportional to the applied loads and thermal gradients. This assumption may not hold for materials subjected to large deformations or high temperatures. The theory is typically formulated under the assumption of small temperature gradients. In situations where temperature changes are large, nonlinear effects may become significant, and the theory may not be accurate.

The modified Green-Lindsay (MG-L) theory is a revised version of the Green-Lindsay (G-L) theory that expands the classical linear thermoelasticity theory. This extended theory applies to extreme conditions, such as high temperatures, rapid heating or cooling, or other scenarios where the assumptions of the original theory may break down. This revised theory considers the impact of nonlinear thermal expansion to provide a more comprehensive description of the thermomechanical behavior of materials. By doing so, the MG-L theory offers improved predictions of the stress and strain in materials that are exposed to significant temperature changes and thermal gradients, which can result in significant mechanical stresses and deformations.

Yu et al. [13] used the extended thermodynamics principle to propose a model of generalized thermoelasticity that incorporates strain rate terms into the Green-Lindsay model. Quintanilla [14] reported some qualitative results for the MG-L thermoelasticity model. Ghodrat et al. [15] developed a numerical method to solve the governing equations for a large deformation domain in an elastic medium exposed to thermal shock under the MG-L theory of thermoelasticity. In the context of MG-L, Sarkar and De [16] examined the propagation of thermoelastic waves and determined that both MG-L and G-L have a significant impact on the amplitude ratios of reflected waves. A study that elaborates the response of a heat source along with thermomechanical loading in a MG-L generalized thermoelastic half-space with non-local and two temperature parameters is presented by Kumar et al. [17].

The non-local theory of thermoelasticity models the non-local effects by introducing a non-local constitutive equation that considers the temperature field over a larger region. This theory is useful in understanding the thermomechanical behavior of materials at small scales, where non-local effects can play a significant role in the material response. A non-local elasticity theory was developed by Eringen and Edelen [18], using global balance laws and the second law of thermodynamics. Initially, the non-local theory of elasticity was used to study screw dislocations and surface waves in solids (Lazar and Agiasofitou [19]).

A new model was discussed by Pramanik and Siddhartha [20] by using Eringen's non-local thermoelasticity theory, which explored the transmission of Rayleigh surface waves in a uniform, isotropic medium. Luo et al. [21] studied the temporary thermoelastic reactions of a slab with thermal properties that rely on the temperature, using a non-local thermoelastic model. In the case of non-local bio-thermoelastic media with diffusion, Kumar et al. [22] developed a dynamic model incorporating the impact of non-local and dual-phase lags.

Malischewsky [23] investigated the propagation of Rayleigh waves using impedance boundary conditions. In the context of thermoelastic medium, Singh [24] examined the reflection of plane waves utilizing impedance boundary conditions. In a study conducted by Kaushal et al. [25], they investigated how diffusion and impedance parameters affect the propagation of plane waves in a thermoelastic medium using both the Green and Lindsay theory (G-L) and the Coupled theory (C-T) of thermoelasticity. Yadav [26] examined the influence of impedance parameters on the reflection of plane waves in a thermoelastic medium subjected to rotating and magnetic effects.

The purpose of the manuscript is to explore propagation of waves in thermoelastic media, which has been a focal point in seismology. Notably, these investigations play a crucial role in mineral ore exploration, hydrocarbon detection, and the planning and construction of infrastructure such as dams, bridges, roads, and highways.

The other authors explored various problems in the field of MG-L but the governing equations for a homogeneous and isotropic thermoelastic medium to determine the amplitude ratios of reflected LD-wave, T-wave, and SV-wave having impacts of non-local and TT under impedance boundary conditions is not explored. In the context of plane wave reflection, the consideration of impedance boundary conditions becomes paramount. These conditions are characterized by linear combinations of unspecified functions and their derivatives along the boundary. Such scenarios are frequently encountered in acoustics, electromagnetism, and seismology. This new model has the potential for application in fields such as geophysics, seismology, and earthquake engineering.

Basic equations

In the present investigation, we consider the MG-L model proposed by Yu et al. [13] along with non-local theory given by Eringen and Edelen [18] and two temperature theory of thermoelasticity given by Youssef [6]. So, in the absence of body forces and heat sources, the field equations and constitutive relations with non-local, TT under MG-L model of thermoelasticity in general cartesian coordinate system $Ox_1x_2x_3$are given as:

$$\left(1+\eta_1\tau_1\frac{\partial}{\partial t}\right)[(\lambda+\mu)\nabla(\nabla\cdot\vec{u})+\mu\nabla^2\vec{u}]-\beta_1\left(1+\eta_2\tau_1\frac{\partial}{\partial t}\right)\nabla T=\rho(1-\xi_1^2\nabla^2)\frac{\partial^2\vec{u}}{\partial t^2}, \tag{1}$$

$$K^*\nabla^2\varphi=\left(1+\eta_3\tau_0\frac{\partial}{\partial t}\right)(\beta_1T_0\dot{u}_{k,k})+\left(1+\eta_4\tau_0\frac{\partial}{\partial t}\right)\rho C_e\dot{T}, \tag{2}$$

$$t_{ij}=\left(1+\eta_1\tau_1\frac{\partial}{\partial t}\right)[\lambda u_{k,k}\delta_{ij}+\mu(u_{i,j}+u_{j,i})]-\beta_1\left(1+\eta_2\tau_1\frac{\partial}{\partial t}\right)T\delta_{ij}, \tag{3}$$

$$T=(1-a\nabla^2)\varphi, \tag{4}$$

where λ, μ -Lame's constants, ξ_1 - non-local parameter, t - time, $\beta_1=(3\lambda+2\mu)\alpha_t$, α_t - coefficient of linear thermal expansion, ρ, C_e - density and specific heat, K^* - thermal conductivity, φ - conductive temperature, T - temperature, t_{ij} - components of stress tensor, τ_0, τ_1- the relaxation times, δ_{ij}- Kronecker delta, $\vec{u}$- displacement vector, T_0- reference temperature, η_1, η_2, η_3, η_4 - constants, a-TT parameter, ∇^2- Laplacian operator.

The Eqs. (1)-(4) reduce to the following:

$\eta_1=\eta_2=\eta_3=\eta_4=1$, Modified Green-Lindsay, (MG-L), (2018).
$\eta_1=\eta_3=0, \eta_2=\eta_4=1$, Green-Lindsay, (G-L), (1972).
$\eta_1=\eta_2=0, \eta_3=\eta_4=1$, Lord-Shulman, (L-S), (1967).
$\eta_1=\eta_2=\eta_3=\eta_4=0$, Coupled thermoelasticity, (C-T), (1980).

Problem statement

A homogeneous, isotropic thermoelastic solid half space with TT and non-local is considered. The rectangular Cartesian coordinate system $Ox_1x_2x_3$is taken such that the origin is located on the surface $x_3 = 0$ and x_3-axis is pointing normally to the medium as shown in Fig. 1.

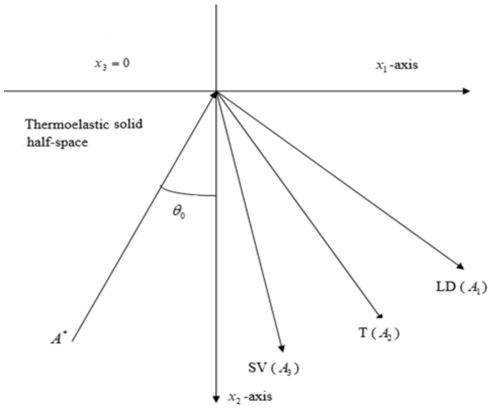

Fig. 1. Geometry of the problem

The components of displacement are taken as follows for a two-dimensional problem:

$$\vec{u} = (u_1, 0, u_3). \tag{5}$$

Dimensionless quantities are referred as:

$$(x_i', u_i') = \frac{\omega_1}{c_1}(x_i, u_i), \qquad t_{3i}' = \frac{t_{3i}}{\beta_1 T_0}, \qquad (\varphi', T') = \frac{1}{T_0}(\varphi, T), \quad (t', \tau_0', \tau_1') = \omega_1(t, \tau_0, \tau_1),$$

$$a' = \frac{\omega_1^2}{c_1^2} a, \qquad {\xi_1}' = \frac{w_1}{c_1}\xi_1, \quad ({z_1}', {z_2}') = \frac{c_1}{\beta_1 T_0}(z_1, z_2), \qquad {z_3}' = \frac{c_1}{K*} z_3, \qquad \iota = 1, 3. \tag{6}$$

where $c_1^2 = \frac{\lambda + 2\mu}{\rho}$ and $\omega_1 = \frac{\rho C_e C_1^2}{K^*}$.

After removing the primes and introducing the values defined by Eq. (6) in addition to Eq. (5), in Eqs. (1)-(4) we get,

$$\left(1 + \eta_1 \tau_1 \frac{\partial}{\partial t}\right)\left[a_1 \frac{\partial e}{\partial x_1} + a_2 \nabla^2 u_1\right] - a_3\left(1 + \eta_2 \tau_1 \frac{\partial}{\partial t}\right)\frac{\partial T}{\partial x_1} = (1 - \xi_1^2 \nabla^2)\frac{\partial^2 u_1}{\partial t^2}, \tag{7}$$

$$\left(1 + \eta_1 \tau_1 \frac{\partial}{\partial t}\right)\left[a_1 \frac{\partial e}{\partial x_3} + a_2 \nabla^2 u_3\right] - a_3\left(1 + \eta_2 \tau_1 \frac{\partial}{\partial t}\right)\frac{\partial T}{\partial x_3} = (1 - \xi_1^2 \nabla^2)\frac{\partial^2 u_3}{\partial t^2}, \tag{8}$$

$$\nabla^2 \varphi = a_4\left(1 + \eta_3 \tau_0 \frac{\partial}{\partial t}\right)\frac{\partial}{\partial t}(u_{1,1} + u_{3,3}) + \left(1 + \eta_4 \tau_0 \frac{\partial}{\partial t}\right)\frac{\partial T}{\partial t}, \tag{9}$$

$$T = (1 - a\nabla^2)\varphi, \tag{10}$$

$$t_{33} = \left(1 + \eta_1 \tau_1 \frac{\partial}{\partial t}\right)\left[a_5 \frac{\partial u_3}{\partial x_3} + a_6 \frac{\partial u_1}{\partial x_1}\right] - \left(1 + \eta_2 \tau_1 \frac{\partial}{\partial t}\right)T, \tag{11}$$

$$t_{31} = \left(1 + \eta_1 \tau_1 \frac{\partial}{\partial t}\right)\left[a_7\left(\frac{\partial u_3}{\partial x_1} + \frac{\partial u_1}{\partial x_3}\right)\right], \tag{12}$$

where

$$a_1 = \frac{\lambda + \mu}{\rho C_1^2}, a_2 = \frac{\mu}{\rho C_1^2}, a_3 = \frac{\beta_1 \tau_0}{\rho C_1^2}, a_4 = \frac{\beta_1 {C_1}^2}{K^* \omega_1}, a_5 = \frac{\lambda + 2\mu}{\beta_1 T_0}, a_6 = \frac{\lambda}{\beta_1 T_0}, a_7 = \frac{\mu}{\beta_1 T_0}, e = \frac{\partial u_1}{\partial x_1} + \frac{\partial u_3}{\partial x_3}.$$

To decouple the above system of equations, we take $u_1$and $u_3$in the dimensionless form as:

$$u_1 = q_{,1} - \psi_{,3}, \qquad u_3 = q_{,3} + \psi_{,1}. \tag{13}$$

Using Eqs. (7)-(10) and (13), we get the following set of equations:

$$\left(1+\eta_1\tau_1\frac{\partial}{\partial t}\right)(\nabla^2 q)-a_3\left(1+\eta_2\tau_1\frac{\partial}{\partial t}\right)T=(1-\xi_1^2\nabla^2)\frac{\partial^2 q}{\partial t^2}, \tag{14}$$

$$a_2(1+\eta_1\tau_1\frac{\partial}{\partial t})(\nabla^2\psi)-(1-\xi_1^2\nabla^2)\frac{\partial^2\psi}{\partial t^2}=0, \tag{15}$$

$$\nabla^2\varphi=a_4\left(1+\eta_3\tau_0\frac{\partial}{\partial t}\right)\frac{\partial}{\partial t}\nabla^2 q+\left(1+\eta_4\tau_0\frac{\partial}{\partial t}\right)\frac{\partial T}{\partial t}. \tag{16}$$

Dispersion equation and its solutions

Assuming the motion to be harmonic and for solving the Eqs. (14)-(16), we assume solutions in the form:

$$(q,\varphi,\psi)=(q^0,\varphi^0,\psi^0)e^{\iota k(x_1 Sin\theta_0-x_3 Cos\theta_0)+\iota\omega t}, \tag{17}$$

where k denotes as wave number, ι is known as iota, θ_0 is angle of inclination and quantities such as q^0,φ^0,ψ^0 are arbitrary constants. Using the values of q,φ,ψ we obtained following equations:

$$(A\nu^4+B\nu^2+C)(q,\varphi)=0, \tag{18}$$

$$(\nu^2-A_1)\psi=0, \tag{19}$$

where A=$E_2\,i\omega$, B=$(E_2 a\omega^3 i+\omega^2)+i\omega E_2(\xi_1^2\omega^2-E_1)-(a_3\,a_4E_3E_4\,i\omega)$, C= $(\xi_1^2\omega^2-E_1)(E_2 a\omega^3 i+\omega^2)-ia a_3a_4E_3E_4\omega^3$, $A_1=\ (1+\eta_1\tau_1\,i\omega)a_2-\xi_1^2\omega^2$, $E_1=(1+\eta_1\tau_1 i\omega)$, $E_2=(1+\eta_4\tau_0 i\omega)$, $E_3=(1+\eta_3\tau_0 i\omega)$, $E_4=(1+\eta_2\tau_1 i\omega)$.

Restriction on boundary

Impedance boundary conditions consist of unknown functions and their derivatives prescribed on the boundary. These conditions find widespread use in multiple disciplines such as thermoelasticity, acoustics, and electromagnetism within the realm of Physics. When dealing with seismic wave interactions involving discontinuities, the typical assumption is an ideally welded contact, ensuring continuity of relevant displacement and stress components. Consequently, it is suitable to treat these contact planes as extremely thin layers, giving rise to boundary conditions similar to impedance conditions. Hence, following Malischewsky [23] and Schoenberg [27], the impedance boundary conditions at $x_3=0$ are:

(i) $t_{33}+\omega z_1 u_3=0$, (ii) $t_{31}+\omega z_2 u_1=0$, (iii) $K^*\frac{\partial T}{\partial x_3}+\omega z_3 T=0$, (20)

where z_1, z_2 and z_3 are impedance parameters, the boundary conditions at free surface can be obtained by setting $z_1=z_2=z_3=0$.

To obtain amplitude ratios, we consider q,φ,ψ as follows:

$$q=\Sigma(A_{0\iota}e^{\iota k_0(x_1 Sin\theta_0-x_3 Cos\theta_0)+\iota\omega t}\ +\ A_\iota e^{\iota k_\iota(x_1 Sin\theta_\iota+x_3 Cos\theta_\iota)+\iota\omega t}), \tag{21}$$

$$\varphi=\Sigma(d_\iota A_{0\iota}e^{\iota k_0(x_1 Sin\theta_0-x_3 Cos\theta_0)+\iota\omega t}+d_\iota A_\iota e^{\iota k_\iota(x_1 Sin\theta_\iota+x_3 Cos\theta_\iota)+\iota\omega t}), \tag{22}$$

$$\psi=(A_{03}e^{\iota k_0(x_1 Sin\theta_0-x_3 Cos\theta_0)+\iota\omega t}+A_3 e^{\iota k_3(x_1 Sin\theta_3+x_3 Cos\theta_3)+\iota\omega t}), \tag{23}$$

where $d_l=\frac{\iota\omega a_4E_3k_l^2}{k_l^2+\iota\omega E_2(1+ak_l^2)}$, ($l$=1,2), $A_{0\iota}$ are the amplitude of incident Longitudinal wave (LD-wave), thermal waves (T-wave) and shear waves (SV-wave). A_ι are the amplitude of the reflected Longitudinal wave (LD-wave) and reflected Thermal waves (T-wave) and A_3 is the amplitude of the reflected Shear wave (SV-wave).

Snell's Law is given as

$$\frac{\sin\theta_0}{v_0} = \frac{\sin\theta_1}{v_1} = \frac{\sin\theta_2}{v_2} = \frac{\sin\theta_3}{v_3}, \tag{24}$$

where

$$k_1 v_1 = k_2 v_2 = k_3 v_3 = \omega, \text{ at } x_3 = 0, \tag{25}$$

$$v_0 = \begin{cases} v_1, \text{for incident LD} - \text{wave} \\ v_2, \text{for incident T} - \text{wave} \\ v_3, \text{for incident SV} - \text{wave} \end{cases}.$$

Using potential defined by Eq. (13) along with Eqs. (21)-(25) in the boundary conditions given by Eq. (20), we obtained a system of equations defined as:

$$\sum a_{ij} R_j = Y_j, (i, j = 1, 2, 3), \tag{26}$$

where $a_{1i} = -[E_1\, a_5 k_i^2 \cos^2\theta_i + E_1 a_6 k_i^2 \sin^2\theta_i + E_4(1 + a k_i^2) d_i + i k_i \cos\theta_i\, w z_1]$,

$a_{13} = (a_6 - a_5) E_1 k_3^2 \sin\theta_3 \cos\theta_3 + i k_3 \sin\theta_3 w z_1$,

$a_{2i} = -2E_1\, a_7 k_i^2 \sin\theta_i \cos\theta_i + i k_i \sin\theta_i\, w z_2$,

$a_{23} = E_1\, a_7 k_3^2 (\cos^2\theta_3 - \sin^2\theta_3) - i k_3 \cos\theta_3\, w z_2$,

$a_{3i} = d_i (1 + a k^2)[i k_i K^* \cos\theta_i + w z_3]$, $i = 1, 2$.

Unique cases

Modified Green-Lindsay model with two temperature. Let $\xi_1 \to 0$ in Eq. (26), we obtain the resulting expression for MG-L theory of thermoelasticity along with TT effect. The results tally with those obtained by Sarkar and Mondal [28].

Non-local modified Green-Lindsay model. As TT parameter vanishes i.e. a=0 in Eq. (26), we obtain the results for MG-L model involving non-local impact.

Non-local G-L generalized thermoelastic model with two temperature. Taking $\eta_1 = \eta_3 = 0, \eta_2 = \eta_4 = 1$, reduces the system of equation defined by Eq. (26) for G-L model having non-local and TT effect.

Non-local L-S generalized thermoelastic model with two temperature. Putting $\eta_1 = \eta_2 = 0, \eta_3 = \eta_4 = 1$, in Eq. (26) will yield the expression for L-S model involving non-local and TT. If we vanish the TT effect then the model reduces to L-S generalized thermoelastic model with non-local effects and the results tally with those obtained by Singh and Bijarnia [29].

Coupled thermoelastic model with non-local and two temperature. Let $\eta_1 = \eta_2 = \eta_3 = \eta_4 = 0$, i.e. in absence of relaxation time, Eq. (26) gives the corresponding expression for CT model along with non-local and TT.

Computational interpretation

To study the effect of various parameters, the numerical calculations are carried out for three different cases, the effect of (i) non-local and impedance parameters (ii) TT and impedance parameters (iii) different theories of thermoelasticity i.e. MG-L, G-L and L-S theories.

Following Dhaliwal and Singh [30], we take the case of magnesium crystal, the physical constants used are: $\lambda = 2.17 \times 10^{10}\ \mathrm{Nm^{-2}}$, $\mu = 3.278 \times 10^{10}\ \mathrm{Nm^{-2}}$, $K^* = 1.7 \times 10^2\ \mathrm{Wm^{-1}deg^{-1}}$, $\omega_1 = 3.58 \times 10^{11}\ \mathrm{s^{-1}}$, $\beta_1 = 2.68 \times 10^6 \mathrm{Nm^{-2}\ deg^{-1}}$, $\rho = 1.74 \times 10^3\ \mathrm{Kgm^{-3}}$, $C_e = 1.04 \times 10^3\ \mathrm{JKg^{-1}deg^{-1}}$, $T_0 = 298\ \mathrm{k}$, $\tau_0 = 0.1\ \mathrm{s}$, $\tau_1 = 0.2\ \mathrm{s}$. The values of impedance parameters for all the cases are $z_1 = 5$, $z_2 = 2$, and $z_3 = 1$.

Non-local effects and impedance parameters. In this case, we consider fixed value of TT parameter as $a = 0.104$ with $0^o \leq \theta_0 \leq 90^o$. Non-local parameter ($\xi_1 = 0.5$) along with TT and impedance parameters (NTI) is represented by a solid Black line. The case of non-local parameter($\xi_1 = 0.5$) along with TT and without impedance parameters (NTWI) is represented by a solid red. The case of absence of non-local parameter, i.e. ($\xi_1 = 0.0$) along with TT and impedance parameter (TI) is represented by a solid Blue line with center symbol 'Δ'. The case of absence of non-local parameter i.e.($\xi_1 = 0.0$) along with TT and without impedance (TWI) is shown by a violet line with center symbol '⋄'.

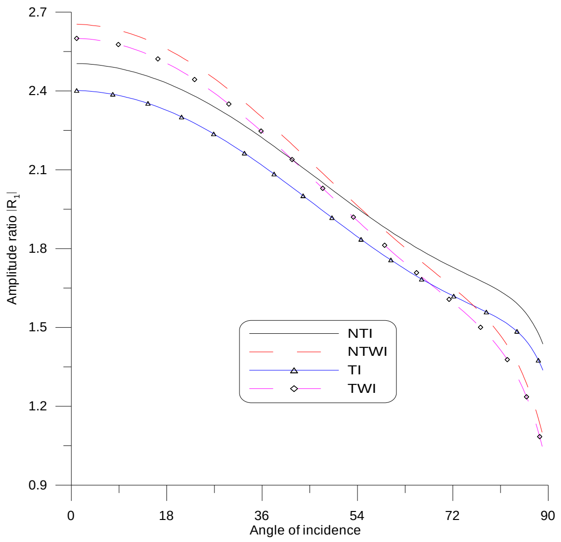

Fig. 2. Variation of Amplitude ratio $|R_1|$
for LD-wave (Impact of non-Local and impedance parameters)

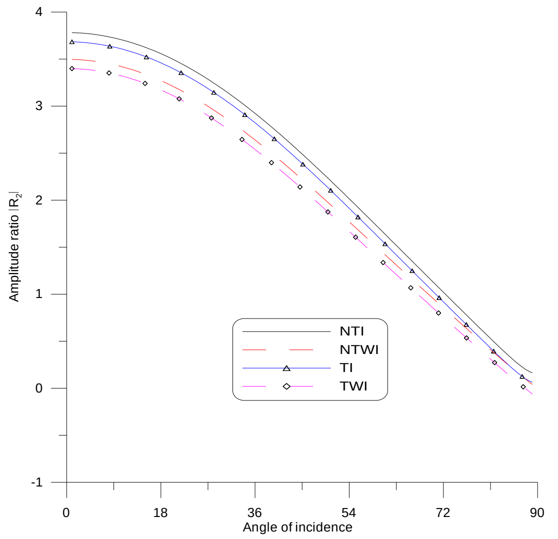

Fig. 3. Variation of Amplitude ratio $|R_2|$
for LD-wave (Impact of non-Local and impedance parameters)

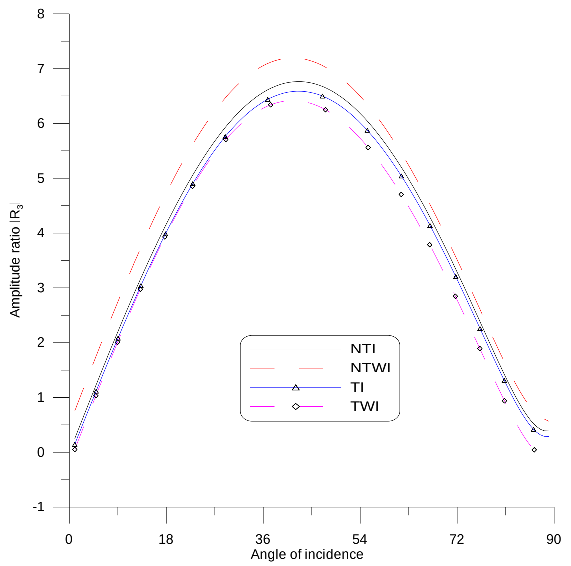

Fig. 4. Variation of Amplitude ratio $|R_3|$
for LD-wave (Impact of non-Local and impedance parameters)

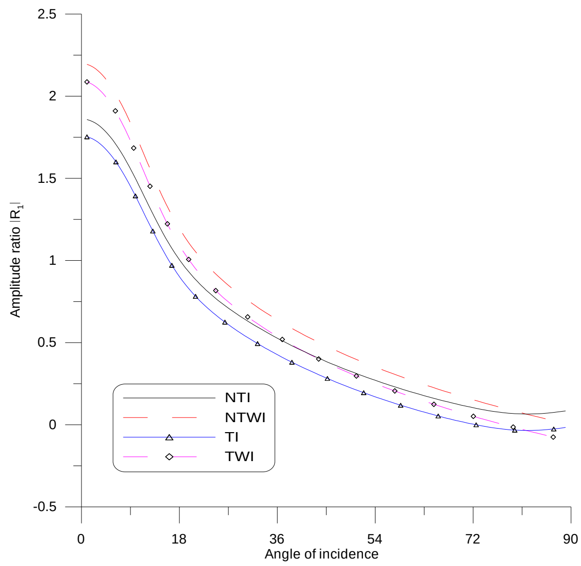

Fig. 5. Variation of Amplitude ratio $|R_1|$
for T-wave (Impact of non-Local and impedance parameters)

LD-wave. In Fig. 2, the changes in $|R_1|$ are depicted as a function of the angle of incidence. It is observed that $|R_1|$ decreases for all the cases considered throughout the entire range. Additionally, it is apparent that $|R_1|$ is more pronounced for the case NTI as compared to TI. Also, the value of $|R_1|$ for the case of NTWI is higher than that of TI, indicating the influence of non-local on$|R_1|$.

Figure 3 illustrates those variations of $|R_2|$ with θ_0, it is noticed that $|R_2|$ decreases for all cases considered, namely NTI, NTWI, TI, and TWI, as θ_0 increases. Specifically, the value of $|R_2|$ for NTI and TI are higher than that of NTWI and TWI respectively, reveals the impact of non-local and impedance on the $|R_2|$.

The trend of variations of $|R_3|$ with θ_0 is shown in Fig. 4. It is observed that the value of $|R_3|$ increases in the first half of the interval and decreases in the remaining range for all considered cases. However, the magnitude of $|R_3|$ is higher for NTWI compared to other cases in the entire range.

T-wave. Figure 5 displays a plot of $|R_1|$ with θ_0, it is evident that $|R_1|$ exhibits a significant downward trend for all the considered cases in the range of $0 \leq \theta \leq 18°$ followed by a steady decline in the remaining interval. Moreover, the magnitude of variations appears to be relatively higher for the NTWI case compared to the other cases throughout the entire range.

Figure 6 illustrates the variations of $|R_2|$ with θ_0, indicating that $|R_2|$ exhibits a downward trend within a range $0 \leq \theta \leq 27°$ for all examined cases. As the values of θ_0 increases further, $|R_2|$ shows a small decrement for all considered cases.

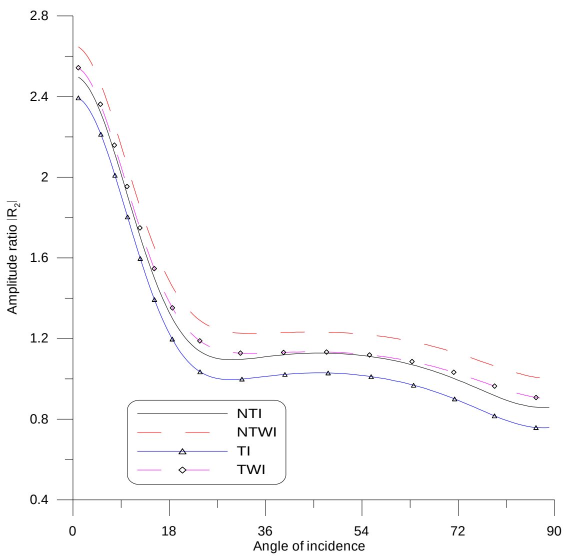

Fig. 6. Variation of Amplitude ratio $|R_2|$ for T-wave (Impact of non-Local and impedance parameters)

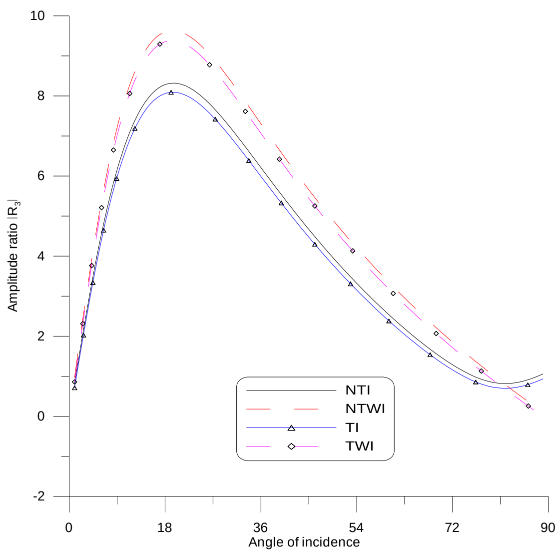

Fig. 7. Variation of Amplitude ratio $|R_3|$ for T-wave (Impact of non-Local and impedance parameters)

From Fig. 7 it is seen that value of $|R_3|$ increases in the interval $0 \leq \theta \leq 18°$ for all considered cases, whereasit exhibits an opposite trend in the remaining range, implying that the amplitude ratio is adversely affected by the impedance parameter. Furthermore, the magnitudes of $|R_3|$ are relatively higher for NTWI, TWI than NTI and TI, which can be attributed to the absence of impedance parameter.

SV-wave. Figure 8 displays a plot of $|R_1|$ with θ_0, indicating that the values of $|R_1|$exhibit an upward trend for all the cases considered with increase in θ_0. It is also seen that magnitude of values for TWI and NTWI are greater as compared to TI and NTI, which reveals the impact of impedance parameter.

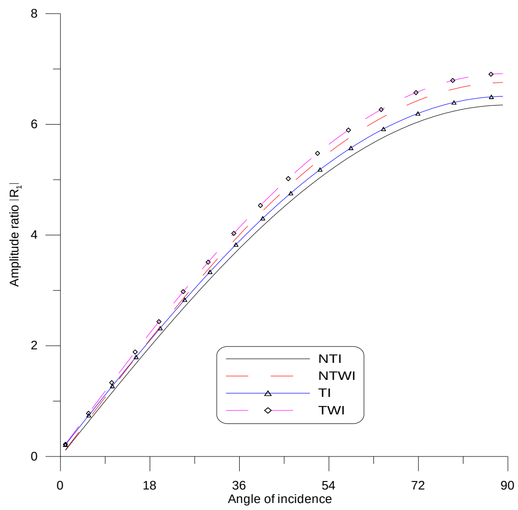

Fig. 8. Variation of Amplitude ratio $|R_1|$ for SV-wave (Impact of non-Local and impedance parameters)

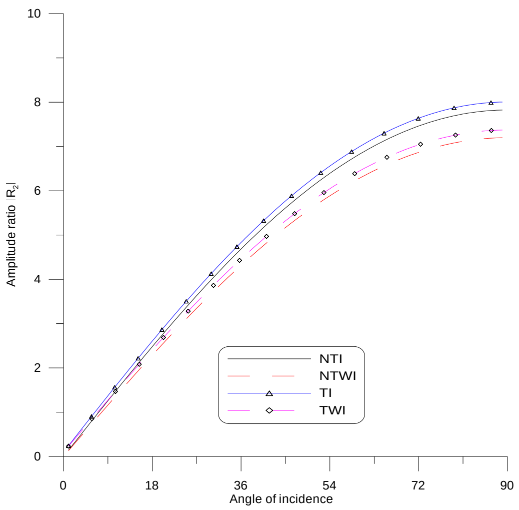

Fig. 9. Variation of Amplitude ratio $|R_2|$ for SV-wave (Impact of non-Local and impedance parameters)

Figure 9 indicates a growing trend of variation of $|R_2|$ in the case of NTI, NTWI, TI and TWI for the entire range. Figure 10 demonstrates that the variations of amplitude ratio $|R_3|$ against θ_0 follows the decreasing trend for all the considered cases in the entire range, magnitude of decrement for NTWI is greater as compared to other cases.

Two temperature effects and impedance parameters. In this case, we consider the fixed value of non-local parameter $(\xi_1 = 0.5)$ parameter and $0^o \leq \theta_0 \leq 90^o$. TT parameter $(a = 0.0104)$ along with non-local and impedance parameters (TNI) is represented by a solid Black line. The TT parameter $(a = 0.0104)$ along with non-local and without impedance parameters (TNWI) is represented by a solid red. The case of absence of TT i.e.$(a = 0.0)$ along with non-local with impedance parameter (NI) is represented by a solid Blue line with center symbol '*Δ*'. The case of absence of TT i.e. $(a = 0.0)$ along with non-local and without impedance (NWI) is represented by a violet with center symbol '⋄'.

LD-wave. From Fig. 11 which is a plot of $|R_1|$ vs θ_0. It is clear that the value of $|R_1|$ follows the descending trend for all the considered cases as θ_0 increases, magnitude of $|R_1|$ for TNI and TNWI are greater than NI and NWI respectively, which reveals the impact of TT parameter.

From Fig. 12, which presents the plot of $|R_2|$ vs θ_0. The graph clearly shows a decline in $|R_2|$ for TNI, TNWI, NI, and NWI. Among these, TNI exhibits the largest variation, while NWI has the smallest. As θ_0 increases, the amplitude ratios eventually converge towards zero value. In Fig. 13, depicts the amplitude ratio $|R_3|$ vs θ_0, demonstrating a positive trend during the first half of the interval, followed by a reversal in the second half for all the cases. Notably, TNWI experiences the largest magnitude of variation, while NWI exhibits the smallest.

T-wave. Figure 14 displays the trend of variations for $|R_1|$ with θ_0. It is observed that the value of $|R_1|$ decreases monotonically throughout the entire range for all considered cases, with varying magnitudes of variation. Moreover, TNI and TNWI are smaller as compared to NI and NWI, which reveals the impact of TT parameter. Figure 15 illustrates the plot of $|R_2|$ against θ_0. It is evident that TNI, NI, TNWI, and NWI exhibit a downward trend for the entire range except for $27 \leq \theta_0 \leq 60$, where $|R_2|$ shows a steady state.

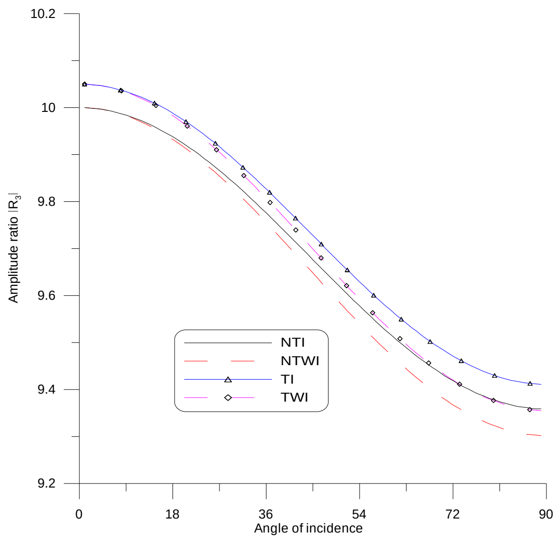

Fig. 10. Variation of Amplitude ratio |R₃| for SV-wave (Impact of non-Local and impedance parameters)

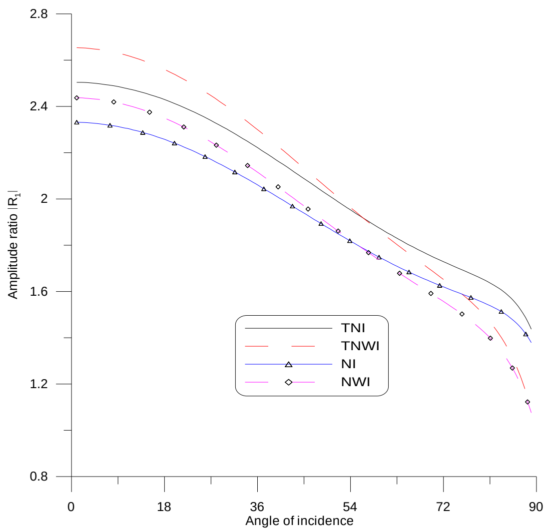

Fig. 11. Variation of Amplitude ratio $|R_1|$ for LD-wave (Impact of TT and impedance parameters)

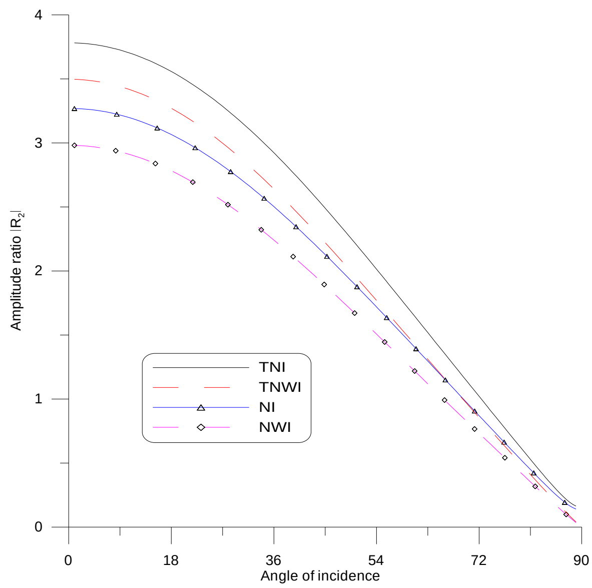

Fig. 12. Variation of Amplitude ratio $|R_2|$ for LD-wave (Impact of TT and impedance parameters)

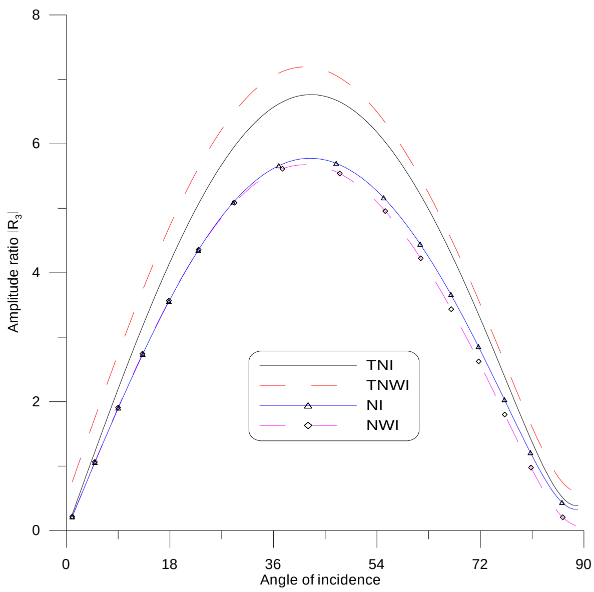

Fig. 13. Variation of Amplitude ratio $|R_3|$ for LD-wave (Impact of TT and impedance parameters)

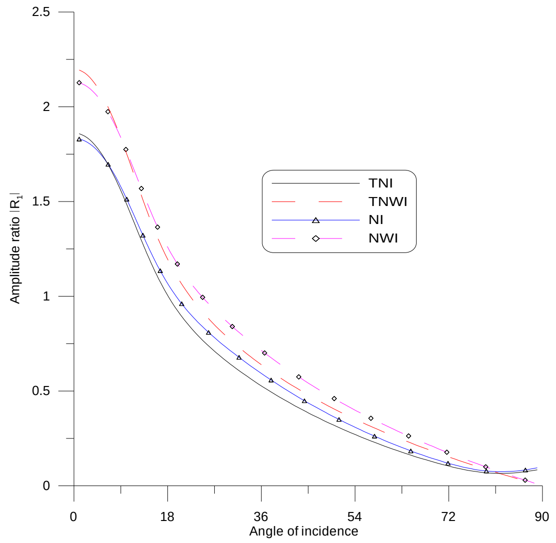

Fig. 14. Variation of Amplitude ratio $|R_1|$ for T-wave (Impact of TT and impedance parameters)

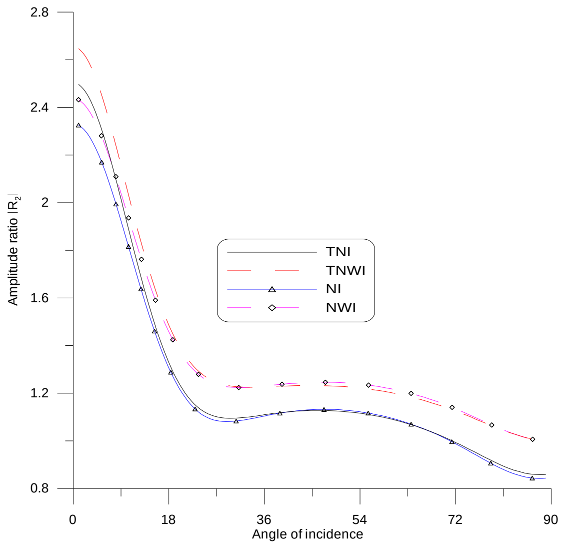

Fig. 15. Variation of Amplitude ratio $|R_2|$ for T-wave (Impact of TT and impedance parameters)

From Fig. 16, which is a plot of $|R_3|$ vs θ_0, it is noticed that $|R_3|$ exhibits an increasing trend in the interval $0 \le \theta \le 18$, and thereafter follows a descending behavior for the remaining range with significant difference in their magnitude.

SV-wave. From Fig. 17, which is a plot of $|R_1|$ vs θ_0. It is clear that the value $|R_1|$ shows an increasing trend in the entire range for all the cases. It is also noticeable that magnitude of variations of $|R_1|$ is larger in case of TNI as compare to TNWI, which reveals impact of impedance. Figure 18 illustrates the plot of $|R_2|$ against θ_0. It indicates the growing trend of variation of $|R_2|$ for all the considered cases with significant difference in magnitude. It is also noticed that the larger variation is seen for TNI as compared to remaining cases. Figure 19 demonstrates a plot of $|R_3|$ vs θ_0, it is seen that impedance has decreasing effect on amplitude ratio $|R_3|$and magnitude of variation is observed larger for the case of NI.

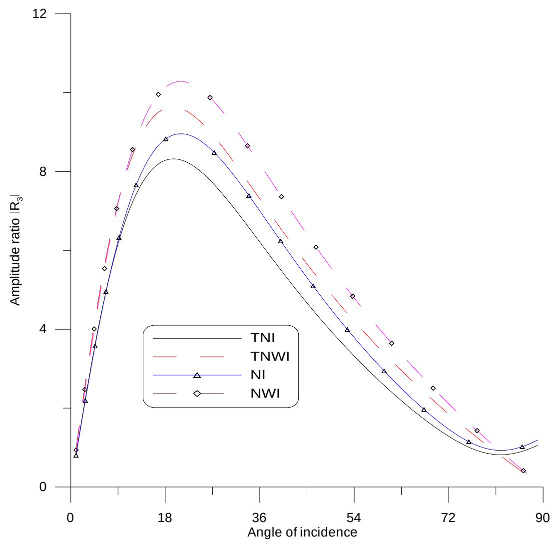

Fig. 16. Variation of Amplitude ratio $|R_3|$ for T-wave (Impact of TT and impedance parameters)

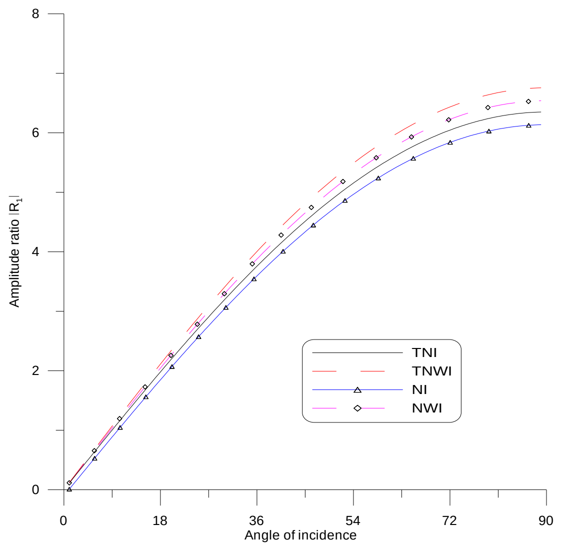

Fig. 17. Variation of Amplitude ratio $|R_1|$ for SV-wave (Impact of TT and impedance parameters)

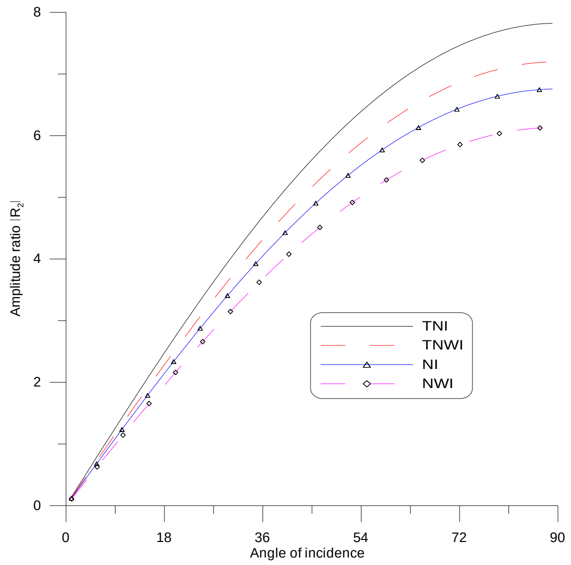

Fig. 18. Variation of Amplitude ratio $|R_2|$ for SV-wave (Impact of TT and impedance parameters)

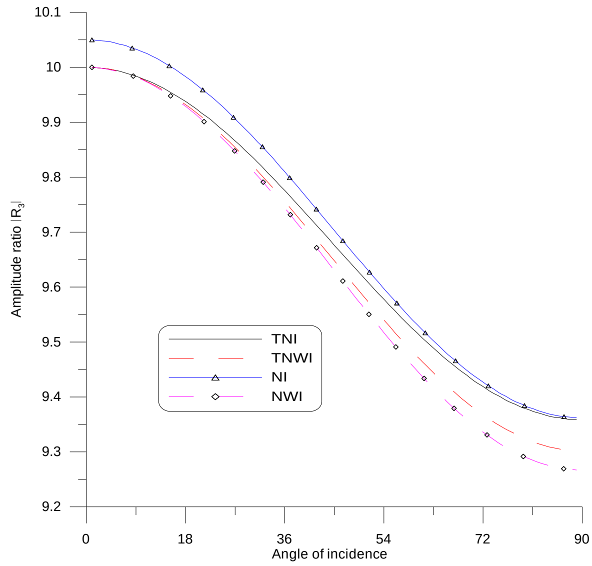

Fig. 19. Variation of Amplitude ratio $|R_3|$ for SV-wave(Impact of TT and impedance parameters)

Different theories of thermoelasticity. LD-wave. Figure 20 depicts the variations of $|R_1|$ vs θ_0. It is noticed that the value of $|R_1|$ shows decreasing trend. Moreover, the value of $|R_1|$ for G-L model is higher as compared with MG-L and L-S model. Figure 21 shows the variation of $|R_2|$ with θ_0. It is seen that $|R_2|$ follows the similar trend as observed for $|R_1|$. Figure 22 illustrates that amplitude ratio $|R_3|$ vs θ_0. It is noticed that the values of $|R_3|$ increases in first half of the interval and in remaining half the values shows a vice-versa trend for all the considered cases.

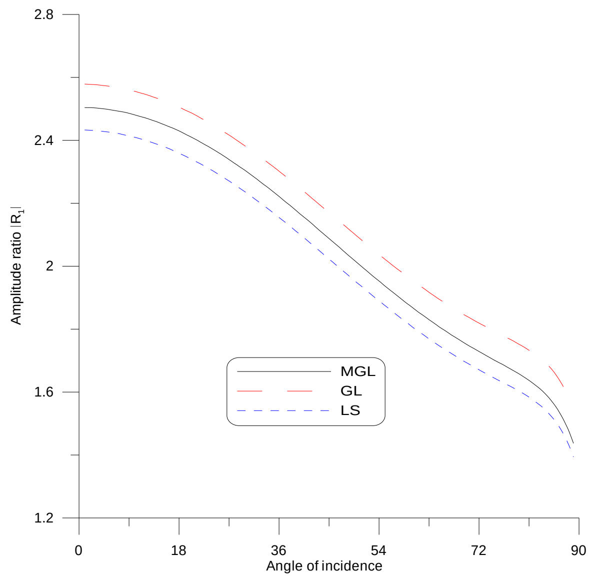

Fig. 20. Variation of Amplitude ratio $|R_1|$ for LD-wave(Impact of Different Theories)

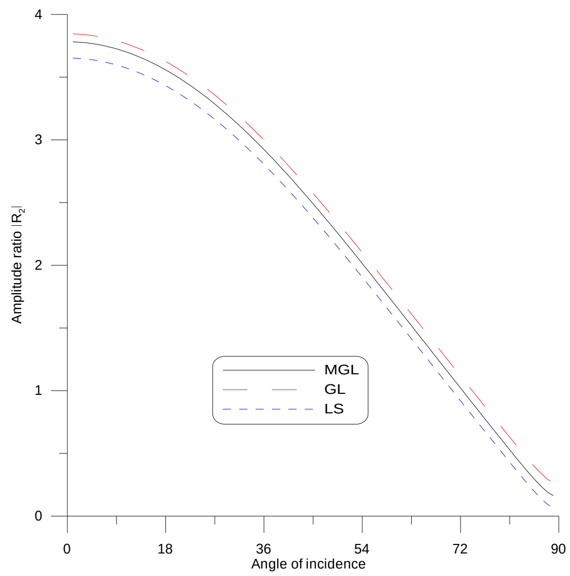

Fig. 21. Variation of Amplitude ratio $|R_2|$ for LD-wave (Impact of Different Theories)

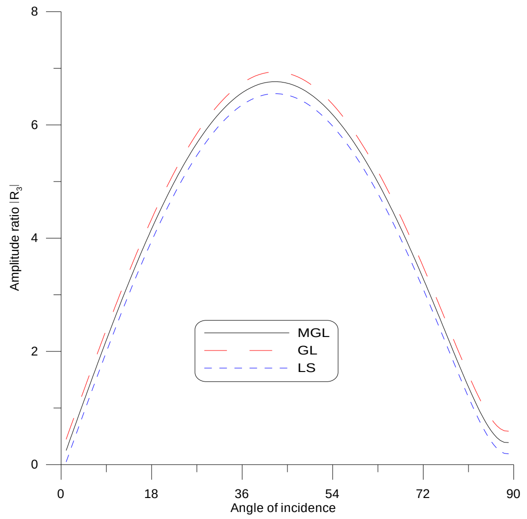

Fig. 22. Variation of Amplitude ratio $|R_3|$ for LD-wave (Impact of Different Theories)

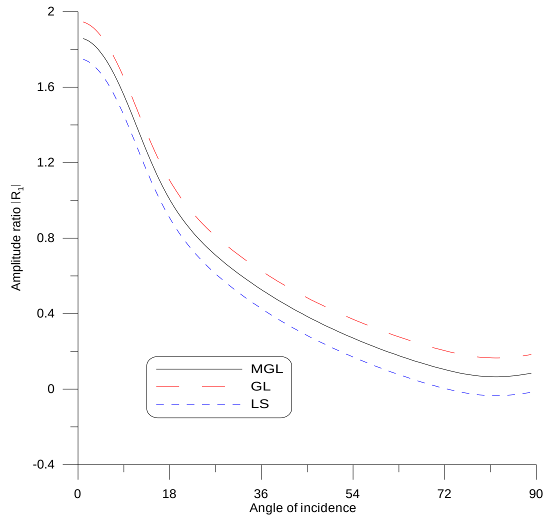

Fig. 23. Variation of Amplitude ratio $|R_1|$ for T-wave (Impact of Different Theories)

T-wave. From Fig. 23, it is observed that the value of $|R_1|$ for MGL, G-L and L-S model follows decreasing trends while magnitude of $|R_1|$ is more for the G-L as compared to MG-L and L-S. From Fig. 24, which is plot of $|R_2|$ vs θ_0. It is noticed that magnitude of $|R_2|$ for G-L is higher as compared to other two models i.e. MG-L model and L-S model. The variations of $|R_3|$ vs $\theta_0$are presented in Fig. 25. It is observed that the value of $|R_3|$ is in upward trend for all considered cases in the range $0 \leq \theta \leq 18^{\circ}$, $\theta \geq 80^{\circ}$ and is in downward trend in rest of the interval.

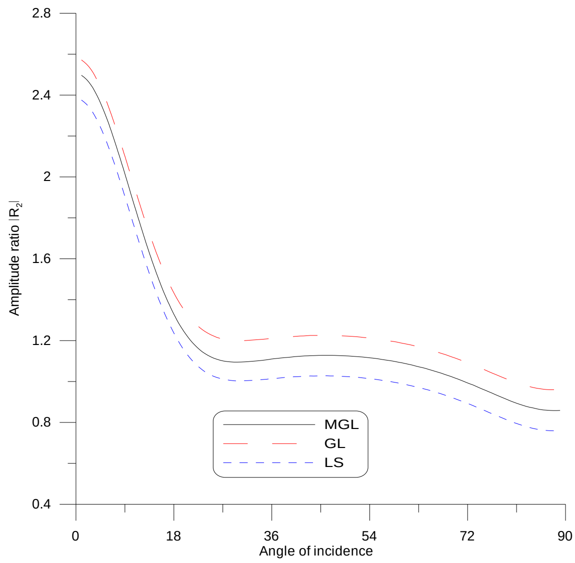

Fig. 24. Variation of Amplitude ratio $|R_2|$ for T-wave(Impact of Different Theories)

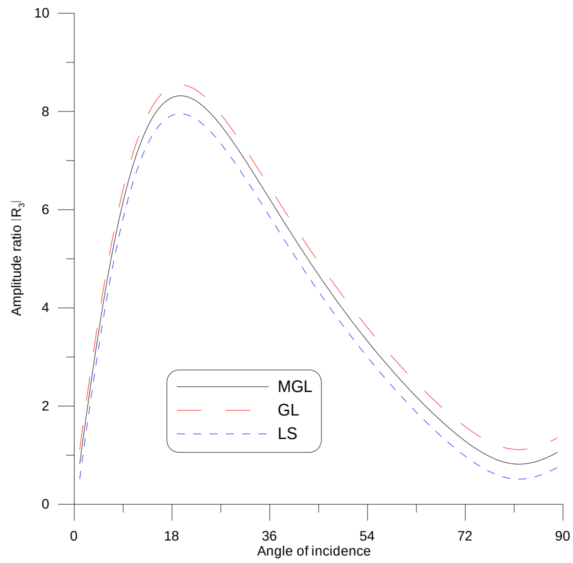

Fig. 25. Variation of Amplitude ratio $|R_3|$ for T-wave (Impact of Different Theories)

SV-Wave. Figure 26 depicts the variations of $|R_1|$ with θ_0. It is observed that the value of $|R_1|$ are in uptrend for all the cases. It is also noticed that the values of $|R_1|$ for G-L model are more as compared to MG-L and L-S model. From Fig. 27, it is observed that the value of $|R_2|$ for G-L, MG-L and L-S follows rising trend for entire range but magnitude of $|R_2|$ for G-L is higher than MG-L, L-S. Figure 28 depicts the variations of $|R_3|$ with θ_0. It is observed that the value of $|R_3|$ follows decreasing trend for all the considered models. Also, the value of $|R_3|$ for G-L model is more as compared to MG-L and L-S model.

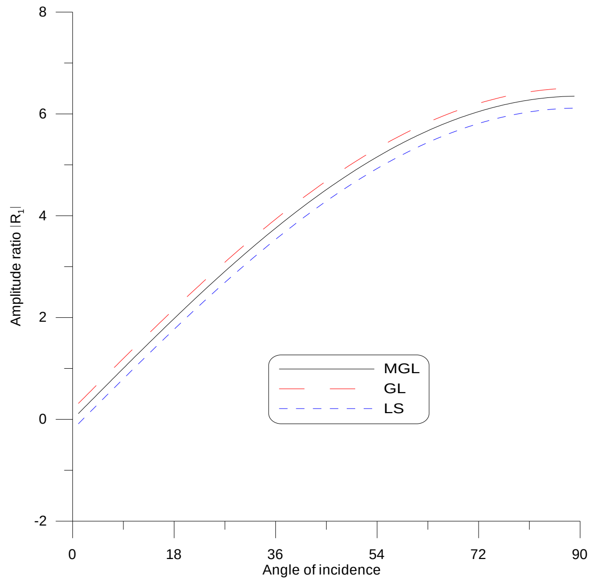

Fig. 26. Variation of Amplitude ratio $|R_1|$ for SV-wave (Impact of Different Theories)

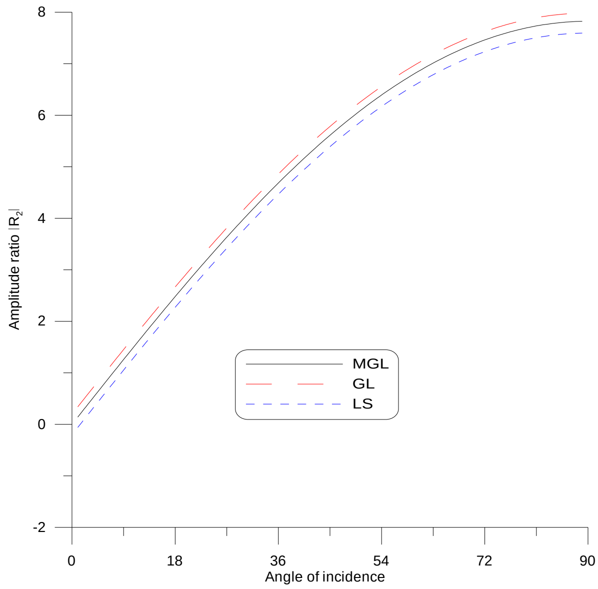

Fig. 27. Variation of Amplitude ratio $|R_2|$ for SV-wave(Impact of Different Theories)

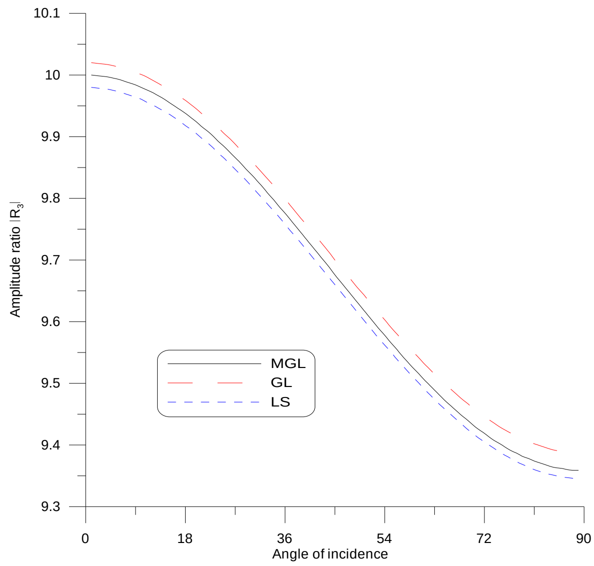

Fig. 28 Variation of Amplitude ratio $|R_3|$ for SV-wave(Impact of Different Theories)

Conclusion

In this investigation, propagation of wave is studied, which is the central focus in seismology, generating precise results applicable to a wide range of economic activities. The amplitude ratios of various reflected waves are obtained by considering a homogenous, isotropic thermoelastic medium under MG-L model of thermoelasticity with the impact of non-local parameter, TT parameter and impedance parameters along with different theories of thermoelasticity. The following results have been obtained:

1. It is observed that for incident LD-wave under the influence of non-local, TT and impedance parameter $|R_1|$ and $|R_2|$ shows a descending behaviour in the entire interval, whereas $|R_3|$ shows uptrend in first half of the interval and thereafter it decreases for all the considered cases.
2. For incident T-wave, the value of $|R_1|$ and $|R_2|$ diminish with increase in θ_0. While $|R_3|$ shows increasing behaviour in the initial range and with increase in θ_0, $|R_3|$ shows downward trend.
3. It is observed that for incident SV-waves, the value of $|R_1|$ and $|R_2|$ continuously increases with increase in θ_0, whereas for $|R_3|$ the values decrease with constant magnitude.
4. It is also seen that for incident LD-wave and T-wave, it is seen that for different theories of thermoelasticity, the values of $|R_1|$ and $|R_2|$ decays with increase in θ_0, whereas for $|R_3|$ the values show uptrend initially and after attaining its maximum point the values of $|R_3|$ decreases. However, in case of incident SV-wave, an opposite behaviour is observed for $|R_1|$ and $|R_2|$ as compared with incident LD-wave and T-wave respectively.
5. The magnitude of $|R_1|$, $|R_2|$, and $|R_3|$ for LD-wave, T-wave, SV-wave in case of G-L model are more as compared with other two models of thermoelasticity.

Based on these findings, it is also concluded that the non-local parameter, TT parameters, and impedance parameters have significant effect on the amplitude ratios as non-local parameter enhances the amplitude ratios for LD-wave and T-wave. It is also observed that amplitude ratios are influenced by different theories of thermoelasticity as the values of amplitude ratios for MG-L are higher than L-S theory and lower than G-L theory of thermoelasticity for all the incident waves. The present new model is useful in developing more accurate representations of thermoelastic solids, making it particularly relevant for geophysical studies, especially in the investigation of seismic events and other phenomena in seismology and engineering.

References

1. Sherief HH, Ezzat MA. A problem in generalized magneto-thermoelasticity for an infinitely long annular cylinder. *Journal of Engineering Mathematics*. 1998;34: 387–402.

2. Ezzat MA, El- Karamany AS, El-Bary AA. Generalized thermo-viscoelasticity with memory-dependent derivatives. *International Journal of Mechanical Sciences*. 2014;89: 470–475.

3. Ezzat MA, El-Bary AA. Effect of variable thermal conductivity and fractional order of heat transfer on a perfect conducting infinitely long hollow cylinder. *International Journal of Thermal Sciences*. 2016;108: 62–69.

4. Shakeriaski F, Ghodrat M, Diaz JE, Behnia M. Recent advances in generalized thermoelasticity theory and the modified models. *Journal of Computational design and Engineering*. 2021;8(1): 15–35.

5. Ezzat MA, Ezzat SM, Alkharraz MY. State-space approach to non-local thermo-viscoelastic piezoelectric materials with fractional dual-phase lag heat transfer. *International Journal of Numerical Methods for heat & Fluid*. 2022;32(12): 3726–3750.

6. Youssef HM. Theory of two-temperature-generalized thermoelasticity. *IMA Journal of Applied Mathematics*. 2013;71(3): 383–390.

7. Ezzat MA, Bary AA. State space approach of two-temperature magneto-thermoelasticity with thermal relaxation in a medium of perfect conductivity. *International Journal of Engineering Science*. 2009;47(4): 618–630.

8. Kaushal S, Kumar R, Miglani A. Wave propagation in temperatures rate dependent thermoelasticity with TT. *Mathematical Sciences*. 2011;5: 125–146.

9. Ezzat MA, El-Bary AA. Magneto-thermoelectric viscoelastic materials with memory-dependent derivative involving two-temperature. *International Journal of Applied Electromagnetic and Mechanics*. 2016;50(4): 549–567.

10. Ezzat MA, El-Karamany AS, El-Bary AA. Two-temperature theory in Green-Naghdi thermoelasticity with fractional phase-lag heat transfer. *Microsystem Technologies*. 2018;24: 951–961.

11. Lofty Kh, El-Bary AA, Sarkar N. Investigation of Rotation on Plane Waves Under Two-Temperature Theory in Generalized Thermoelasticity. *Journal of Applied Mechanics and Technical Physics*. 2022;63(3): 448–457.

12. Al-Lehaibi EAN. The variationally principle of two temperature thermoelasticity in the absence of the energy dissipation theorem. *Journal of Umm Al-Qura University for Engineering and Architecture*. 2022;13: 81–85.
13. Yu YJ, Xue Z , Tian X. A modified Green–Lindsay thermoelasticity with strain rate to eliminate the discontinuity. *Meccanica*. 2018;53: 2543–2554.
14. Quintanilla R. Some qualitative results for a modification of the Green-Lindsay thermoelasticity. *Meccanica*. 2018;53(14): 3607–3613.
15. Ghodrat M, Shakeriaski F, Diaz JE, Mehnia B. Modified Green-Lindsay thermoelasticity wave propagation in elastic materials under thermal shocks. *Engineering J. Comput. Des. Eng*. 2021:8(1): 36-54.
16. Sarkar N, Soumen De. Waves in magneto-thermoelastic solids under modified Green-Lindsay model. *Journal of Thermal Stresses*. 2019;43(5): 594–611.
17. Kumar R, Kaushal S, Sharma G. Mathematical model for the deformation in a Modified Green- Lindsay thermoelastic medium with non-local and two-temperature effects. *Journal of Applied Mechanics and Technical Physics*. 2022;63: 448–457.
18. Eringen AC, Edelen DGB. On nonlocal elasticity. *International Journal of Eng. Science*. 1972;10(3): 233–248.
19. Lazar M, Agiasofitou E. Screw dislocation in non-local anisotropic elasticity. *International Journal of Eng. Science*. 2011;49(12): 1404–1414.
20. Pramanik AS, Siddhartha BS. Surface waves in non-local thermoelastic medium with state space approach. *Journal of Thermal Stresses*. 2020;43(6): 667–686.
21. Luo P, Li X, Tian X. Non-local thermoelasticity and its application in thermoelastic problem with temperature-dependent thermal conductivity. *European Journal of Mechanics - A/Solids*. 2021;87: 104204.
22. Kumar R, Ghangas S, Vashishth AK. Fundamental and plane wave solutions in non-local bio-thermoelasticity diffusion theory. *Coupled Systems Mechanics*. 2021;10(1): 21–38.
23. Malischewsky PG. *Surface Waves and Discontinuities*. Amsterdam: Elsevier; 1987.
24. Singh B. Reflection of elastic waves from plane surface of a half-space with impedance boundary conditions. *Geosciences Research*. 2017;2(4): 242–253.
25. Kaushal S, Kumar R, Parmar K. Influence of diffusion and impedance parameters on wave propagation in thermoelastic medium. *International Journal of Applied Mechanics and Engineering*. 2021;26(4): 99–112.
26. Yadav AK. Effect of Impedance Boundary on the Reflection of Plane Waves in Fraction-Order Thermoelasticity in an Initially Stressed Rotating Half-Space with a Magnetic Field. *International Journal of Thermophysics*. 2021;42: 3.
27. Schoenberg M. Transmission and reflection of plane waves at an elastic viscoelastic interface. *Geophysical Journal International*. 1971;25(1-3): 35–47.
28. Sarkar N, Mondal S. Thermoelastic plane waves under the modified Green-Lindsay model with two temperature formulation. *ZAMM*. 2020;100(11): e201900267.
29. Singh B, Bijarnia R. Non-local effects on propagation of waves in a generalized thermoelastic solid half space. *Structural Engineering and Mechanics*. 2021;77(4): 473–479.
30. Dhaliwal RS, Singh A. *Dynamic Coupled Thermoelasticity*. New Delhi, India: Hindustan Publication Corporation; 1980.

About Authors

Kaushal Sachin Sc

Sachin Kaushal born on 27th April 1984, did M. Sc (2006) from Guru Nanak Dev University (G.N.D.U.), Amritsar (Punjab). Completed Ph. D. (2012) on the topic of "Some Dynamic problems in micropolar thermoelastic media", from C.D.L. University (Sirsa). 2 students are awarded Ph.D. degrees, and 5 students are doing Ph.D. under his supervision. He has 40 papers published, communicated 5 research papers and 5 are ready to publish in the Journals of International repute. He is a reviewer of many International journals.

Kumar Rajneesh

Rajneesh Kumar born on 08th June 1958, received his M.Sc. (1980) from Guru Nanak Dev University (G.N.D.U.), Amritsar (Punjab), M. Phil (1982) from Kurukshetra University Kurukshetra (K.U.K.) and Ph. D. (1986) in Applied Mathematics from Guru Nanak Dev University (G.N.D.U.), Amritsar. Guided 56 M.Phil. students, 21 students were awarded Ph.D. degrees and 9 students are doing Ph.D. under his supervision. He has 621 papers published in the Journal of International repute. His area of research work is Continuum Mechanics (Micropolar elasticity, thermoelasticity, poroelasticity, magnetoelasticity, micropolar porous couple stress theory, viscoelasticity, mechanics of fluid). He is a reviewer of many reputed journals.

Bala Indu Sc

Indu Bala born on 4th April 2001, did M. Sc (2023) from Lovely Professional University, presently pursuing Ph.D. from Lovely Professional University (Phagwara). She has communicated 3 research papers and 1 is ready to publish in the Journal of International repute.

Sharma Gulshan Sc

Gulshan Sharma did MSc Mathematics in 2002, qualified CSIR NET In June 2003. He has a teaching experience of 20 years, presently is an HoD of PG Department of Mathematics Doaba College.